

# CFD SIMULATION OF THE DEPARTURE FROM NUCLEATE BOILING

**Ladislav Vyskocil and Jiri Macek**

UJV Rez a. s., Dept. of Safety Analyses,  
Hlavni 130, 250 68 Husinec – Rez, Czech Republic  
Ladislav.Vyskocil@ujv.cz; Jiri.Macek@ujv.cz

## ABSTRACT

This paper presents an attempt to use multiphase CFD code for prediction of the Departure from Nucleate Boiling (DNB) type of Critical Heat Flux (CHF). Numerical simulations of DNB in boiling flow in vertical tube were performed with the NEPTUNE\_CFD V2 code. This code can simulate multi-component multiphase flow by solving three balance equations for each phase or fluid component. A new set of validated models of physical phenomena in boiling bubbly flow was used in the calculations. Simulated cases were based on data from the Standard tables of CHF in pipes, produced by the Russian Academy of Sciences. It was found out that local DNB criterion based on void fraction equal to 0.8 does not work well with the new set of physical models implemented in NEPTUNE\_CFD V2 code. But it was discovered that the criterion for DNB prediction can be based on the ratio of evaporation heat flux and total wall heat flux. Evaporation heat flux is calculated by the extended Kurul and Podowski wall boiling model. The proposed method of DNB detection was tested on four different pressure levels (13.7 MPa, 15.7 MPa, 17.6 MPa and 19.6 MPa) and it worked well in many cases. The method does not work for low mass flux cases ( $1000 \text{ kg/m}^2/\text{s}$  or  $750 \text{ kg/m}^2/\text{s}$  and below, depending on pressure). Problems with numerical stability were encountered in cases with extremely high critical heat flux. Presented work was carried out within the 7<sup>th</sup> FP EURATOM NURES SAFE project.

## KEYWORDS

Computational fluid dynamics, convective boiling flow, departure from nucleate boiling, critical heat flux, NEPTUNE\_CFD code

## 1. INTRODUCTION

Convective subcooled boiling on the heated wall is being used in many industrial applications. The advantage of subcooled boiling over the other methods of heat removal is a high heat transfer coefficient – due to the large amount of energy associated with the latent heat transfer and also due to the efficient local unsteady cooling of heated wall by liquid during bubble departure. Subcooled boiling can be used for removing of high heat flux ( $10^4 - 10^7 \text{ W/m}^2$ ) from the wall at relatively small temperature difference.

This efficient heat transfer mechanism, however, is limited by a critical heat flux (CHF). Above the critical heat flux, benign nucleate boiling is transformed to a film boiling of poor heat transfer. In a heat-flux-controlled system, this transition of boiling mechanism is characterized by a sudden rise of surface temperature due to the drop of heat transfer coefficient. The rise of the temperature is so high that it can lead to the destruction of the heated surface.

Determination of the critical heat flux is one of the important issues in nuclear reactor safety. In the nuclear reactor core, critical heat flux condition must not occur under any circumstances. The value of critical heat flux depends on the parameters of the coolant and also on the geometry of the channel in fuel

assembly. Critical heat flux performance of the fuel assembly can be improved if the mixing vanes are added to the spacer grids. These mixing vanes generate secondary flow structures (swirl, cross-flow) that increase the mixing and turbulence in the channel. Thus, fuel assembly can be operated safely at higher power. To maximize benefit of the vanes, their size, shape, bend angle and location must be optimized. A series of very expensive experiments is required so as to find out the optimal design of the mixing vanes with respect to CHF and to the pressure drop. With the advent of new generation codes and the increase of the available computational power, it is believed that progress could be made by using Computational Fluid Dynamics (CFD) in nuclear fuel design. Since the optimum spacer grid design should consider a large number of shapes and sizes of mixing vanes, the use of CFD methods would be very useful for selection of better grid spacer designs for the final experimental verification. CFD simulations could supplement or even replace the expensive experiments and reduce the development costs.

In the past, a large number of correlations for calculation of CHF in fuel assemblies were developed. These correlations are based on experimental data and are commonly used in one-dimensional computational codes. Such a correlation can be used only for one geometry (tube, rod bundle) which is given a priori. The same problem applies to the CHF Look-up Tables. So as to perform simulation of boiling flow with critical heat flux in arbitrary geometry, the use of CFD methods seems to be inevitable. CFD simulation of two-phase flow and especially boiling flow is very challenging, however.

This paper presents an attempt to use multiphase CFD code for prediction of the Departure from Nucleate Boiling (DNB) type of Critical Heat Flux. The new version of multiphase code NEPTUNE\_CFD V2.0.1 [1-2] was used for all numerical simulations. This code can simulate multi-component multiphase flow by solving three balance equations for each phase or fluid component. A new set of validated models of physical phenomena in boiling bubbly flow was used in the calculations. Simulated cases were based on data from the Standard tables of CHF in pipes [3-4], produced by the Russian Academy of Sciences. A simple criterion for prediction of CHF from local parameters was proposed. This criterion is based on wall heat flux splitting. The criterion was tested on a large number of cases and the results are provided in a set of tables.

## **2. TABLES OF CRITICAL HEAT FLUX IN TUBES**

The ability of NEPTUNE\_CFD code to simulate convective boiling flow with critical heat flux was tested on selected cases from the tables of CHF in tubes produced by the Russian Academy of Sciences [3-4]. These tables provide critical heat flux as a function of the local bulk mean water condition and for various pressures and mass velocities for fixed tube diameter of 8 mm. See Tables III-VI in chapter 4.7 which are extracted from the tables of CHF [3-4]. The data are valid for heated length/diameter ratio  $L/D \geq 20$ . For tube diameters other than 8 mm the critical heat flux is given by the approximate relationship.

### **2.1. Problem with Distinguishing DNB and Dryout Data Points**

In CHF tables [3-4], departure-from-nucleate-boiling (DNB) data points are not distinguished from dryout data points. Boiling model which is used in this work assumes bubbly flow with DNB-type of boiling crisis. Using this model for dryout data points is not physically meaningful. Therefore, it is necessary to select only DNB data points for our simulations. Unfortunately, it is not completely clear how to distinguish between these two types of boiling crisis.

We assume that the dryout type of boiling crisis occurs only in annular flow. Then we can use two-phase flow regime map for distinguishing DNB data points from dryout data points. In our work, two-phase flow regime map by Hewitt and Roberts [5-6] was used for selection of DNB data points from the CHF tables. Data shown in Tables III-VI are DNB cases according to the map by Hewitt and Roberts.

### 3. MODELLING OF CONVECTIVE BOILING FLOW UNDER CHF CONDITIONS

The work presented in this document follows our previous attempts [7-8] at simulating CHF in CFD code NEPTUNE. In our previous work [7-8], two equation model of turbulence (k-epsilon model liquid) was used with single phase wall functions in all the simulations of CHF. Criterion for prediction of CHF from local parameters was based on local void fraction equal to 0.8.

In our work presented here, we tried to use the best models of physical phenomena in boiling flow which are currently available. It was soon discovered that the results obtained with new models are different from our previous experience. The modeling approach for simulation of convective boiling flow with critical heat flux is described below. It is almost the same as the modeling approach described in the validation manual [9] for the NEPTUNE\_CFD V2 code. Only difference is the wall lubrication force which is used in the manual [9] but not in our work.

The modeling approach is as follows. Two phases are modeled. The primary phase is liquid and the secondary is vapor bubbles. The averaged balance equations for continuity, momentum and energy are solved for each phase (two-fluid model). The same pressure is shared by the two phases.

The  $R_{ij}$ -epsilon SSG [10] model with turbulence reverse coupling (influence of the bubbles on the liquid) is used for modeling the liquid turbulence; the flow of vapor is assumed to be laminar.  $R_{ij}$ -epsilon SSG model is the second order turbulence model based on Reynolds Stress Model solved in the liquid phase. SSG stands for the names of the authors of the original paper [11] – Speziale, Sarkar and Gatski. It is believed that second order turbulence model is more appropriate for the simulation of critical heat flux in the reactor core than two-equation turbulence models because it stands a better chance to predict secondary fluid motions (e.g. behind mixing vanes).

Boiling wall function developed by Mimouni et al. [10] is used in our work instead of previously used single phase wall functions. This boiling wall function can provide better prediction of velocity profiles near the heated wall.

The extended Kurul-Podowski wall-heat-flux-splitting model [8] is used for the simulation of subcooled boiling. This model can be used even when the void fraction at the wall is very high. This might be the case if the critical heat flux is reached. Downstream of the onset of nucleate boiling, the wall heat flux is split into four parts: single phase liquid heat flux, quenching heat flux, evaporation heat flux and vapor superheating heat flux. Fluid properties in this model are taken from distance from the wall equal to the bubble departure diameter. The bubble departure diameter is calculated from the correlation by Ünal [12].

Interfacial momentum transfer is modeled by four following forces.

- Drag force is modeled by the Ishii correlation [13]. This correlation was created for bubbly flows. Drag coefficient calculation is based on the local flow regime.
- Added mass force is modeled by the Zuber correlation [14]. This model for added mass coefficient takes into account the effect of the bubbles concentration.
- Interfacial lift force is modeled by the Tomiyama correlation [15]. This model is applicable not only to spherical bubbles but also to larger-scale deformable bubbles in the ellipsoidal and spherical cap regimes. The correlation predicts the cross-over point in bubble size at which particle distortion causes a reversal of the sign of the lift force.

- Turbulent dispersion force is modeled by the generalized turbulent dispersion model [1-2]. This model calculates the turbulent dispersion coefficient from the drag force and the virtual mass force.

Wall lubrication force is not modeled in our simulations. It was decided not to use this force because determination of wall distance in more complicated geometry would be difficult. Of course, in simulation of circular pipe, calculation of wall distance is simple.

Interfacial heat transfer is divided into two parts.

- Interface to liquid heat transfer is modeled by “bubble model for liquid” [1-2]. This model is recommended for a monodispersed bubble field. Two states are taken into account: a subcooled state as an extension of the Ranz-Marshall model and an overheated state.
- Interface to vapor heat transfer is modeled by the “relaxation time” method [1-2].

Interfacial mass transfer is directly related to interfacial heat transfer.

Distribution of the mean bubble diameter in the flow is modeled by a one-group interfacial area transport equation with models for bubble coalescence and break-up by Ruyer and Seiler [16].

The physical properties of water (liquid and vapor) are calculated by the CATHARE tables.

Criterion for prediction of CHF from local parameters is different from our previous work [7-8]. The new criterion is based on wall heat flux splitting and it is described in section 4.6.

#### 4. SIMULATION OF SELECTED DATA POINTS FROM THE CHF TABLES

Selected data points from the CHF tables [3-4] were simulated in NEPTUNE\_CFD V2 code. In this chapter we will present the computational domain and grid, boundary conditions and calculation procedure. Results from one case will be presented in detail. A new criterion for prediction of CHF from the local parameters will be proposed and tested on a large number of cases. Summary of the results will be provided at the end of this chapter.

##### 4.1. Computational Domain and Mesh

CHF tables [3-4] are given for tubes of 8 mm diameter bore. In most calculations, 1 m long heated section was used. In some extreme cases (high outlet subcooling), inlet parameters for 1 m long heated section would be below the freezing point of water. If this happens, shorter heated section is used – 0.8 m or 0.5 m long. Inlet and outlet adiabatic sections remain the same - 0.5 m long.

Computational domain covers 10° wedge section of a tube confined by symmetry planes and portion of wall. Resolution of the base grid is 20 x (250+500+250) cells for 0.5 m long inlet adiabatic section, 1 m long heated section and 0.5 m long outlet adiabatic section (Fig. 1). First row of cells on the wall is 0.1 mm thin. Boundary layer consists of 5 rows of cells with growth factor of 1.2.

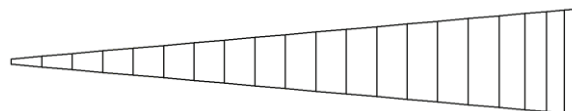


Figure 1. Computational grid – horizontal cross section.

Due to stability reasons, wedge cells in the tube center were omitted and replaced by small symmetry plane. Several other coarse and fine meshes were created for the testing of the grid independence of the results (see section 4.5).

## 4.2. Boundary Conditions

Mass flow rate, temperature and zero void fraction are specified at inlet. Inlet turbulence quantities are calculated by NEPTUNE code from the specified hydraulic diameter. Heat flux is adjusted at the heated wall. Constant static pressure boundary condition is used at outlet. Outlet pressure is set equal to the pressure from the CHF tables.

## 4.3. Calculation Procedure

Pressure, mass flux, exit equilibrium steam quality and critical heat flux are given from the CHF tables [3-4] for every case. Inlet temperature is calculated from these data and for 1 m tube length. If calculated inlet temperature is below freezing point, shorter heated length is used.

Unsteady simulation is started with wall heat flux equal to CHF from the tables. When the flow rate (liquid + vapor) leaving the domain is equal to the inlet flow rate and the wall temperatures and other parameters are stabilized, results are analyzed. Depending on the results, wall heat flux is then decreased or increased so as to find out the interval of the wall heat fluxes in which criterion for CHF is reached.

In some cases (high mass flux, high critical heat flux), it is necessary to begin simulation with a smaller wall heat flux (10-50% of critical heat flux) and let the solution stabilize. After that the heat flux can be increased to CHF. Without this initialization, simulation would become unstable and crash.

## 4.4. Detailed Results for One Data Point

Results for the data point ( $p = 15.7$  MPa,  $G = 2000$  kg/m<sup>2</sup>/s,  $X_{eq} = 0$ ,  $D = 8$  mm, CHF = 2.45 MW/m<sup>2</sup>, see Table IV) will be presented in detail. This case will be referred to as Case 1.

From the exit conditions and the critical heat flux, inlet temperature was calculated for 1 m long heated section. The calculated inlet temperature is 510.1 K which is well above the freezing point and the use of shorter heated section is not necessary.

Fig. 2 and Fig. 3 show the results of the Case 1 when wall heat flux in the simulation is equal to CHF from the tables. Computational domain in Fig. 2 is stretched in horizontal direction (30:1 scale) for the visualization. Actual domain is 2 m long and 4 mm wide. Vapor superheating heat flux in Case 1 is negligible and it is not shown in Fig.3. Note that maximum void fraction is about 38% (Fig. 2a). This result is very different from our previous simulations of CHF [7-8] with older version of NEPTUNE and different set of physical models where the maximum void fraction was very high (80%) at critical heat flux conditions. Similar or even lower void fractions were observed in many other simulated cases. It is clear that with the current modeling approach, the CHF criterion cannot be based on critical void fraction equal to 80%. A new local CHF criterion was proposed, see section 4.6.

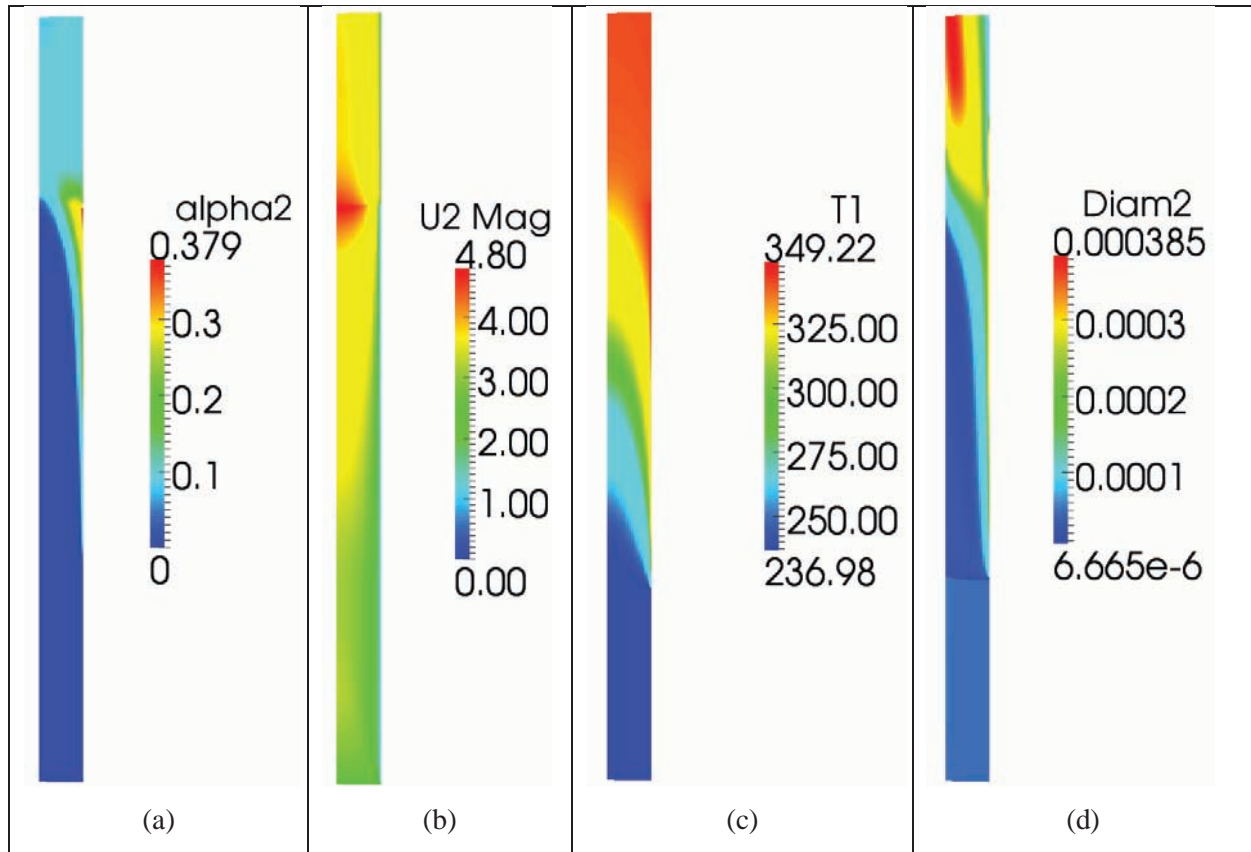


Figure 2. Case 1: (a) void fraction [-], (b) vapor velocity [m/s], (c) liquid temperature [°C] and (d) mean bubble diameter [m].

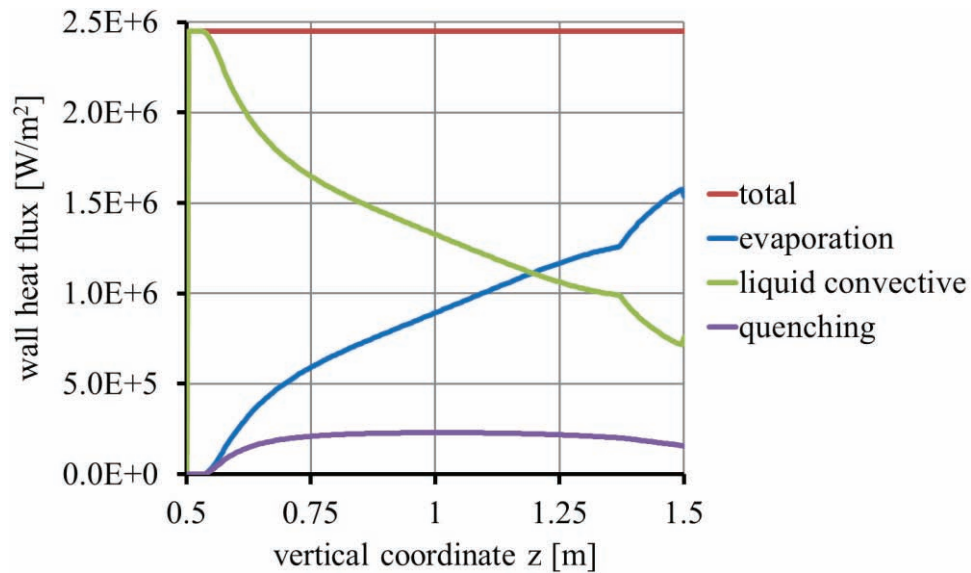


Figure 3. Case 1: wall heat flux splitting.

#### 4.5. Test of Solution Grid Independence

The base grid described in section 4.1 has resolution similar to fine meshes from the NEPTUNE validation cases [9]. Nevertheless, several other meshes were created so as to check the solution grid independence. Results from the Case 1 calculated on four different meshes are compared in Fig. 3.

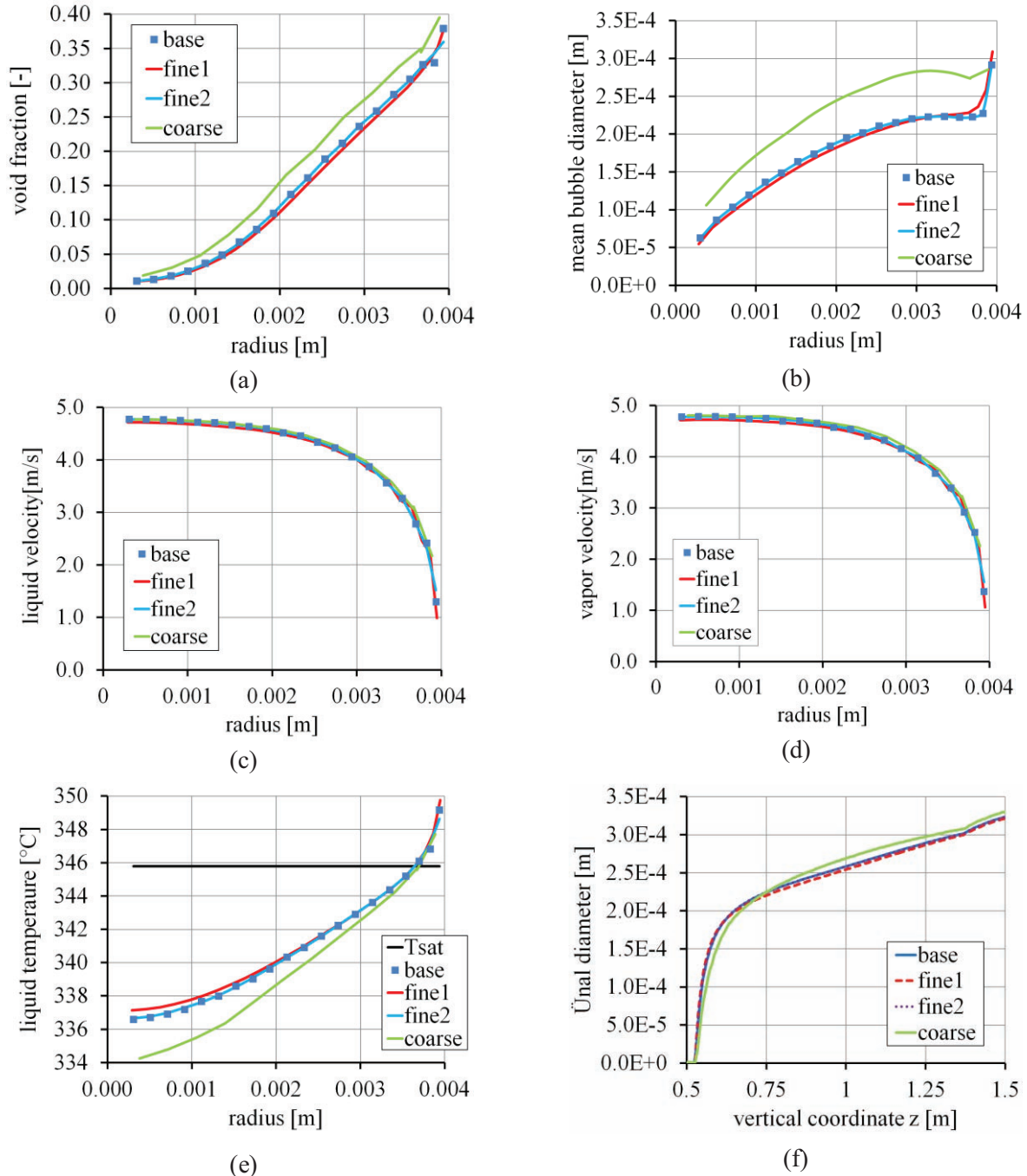


Figure 3. Case 1: Test of solution grid independence. Calculated profiles of flow variables at the end of heated section (a-e) and bubble departure diameter along the tube height (f).

Resolution of meshes in Fig. 3 is as follows:

coarse mesh: 12 x (250+500+250) cells, 0.2 mm thin wall-adjacent cells  
 base mesh: 20 x (250+500+250) cells, 0.1 mm thin wall-adjacent cells  
 fine1 mesh: 24 x (300+600+300) cells, 0.075 mm thin wall-adjacent cells  
 fine2 mesh: 20 x (1000+2000+1000) cells, 0.1 mm thin wall-adjacent cells

The use of finer boundary layer than that in the “fine1” mesh leads to problems with stability of the numerical solution. It was concluded that the base mesh is fine enough for the demonstration of the method. Because many cases have to be calculated, it is not reasonable to use too fine mesh.

#### 4.6. New Criterion for Prediction of CHF from the Local Parameters

Many different cases were calculated and it was found out that the CHF criterion based on void fraction = 80% does not work well with new models in NEPTUNE\_CFD V2. But it was discovered that the CHF criterion can be based on ratio of [evaporation heat flux/total wall heat flux]. This ratio will be referred as “ $q_e/q_w$ ”. Evaporation heat flux is one of 4 heat fluxes calculated by the extended Kurul and Podowski wall boiling model [8]. Fig. 4 shows what happens with  $q_e/q_w$  ratio when total wall heat flux in Case 1 is increased from 90% of CHF value from the tables to CHF value. Reasonable predictions of critical heat flux for pressure level of 15.7 MPa can be obtained if the critical value of  $q_e/q_w$  ratio is set to 0.57. This value is different for different pressures. Method was tested on cases at four different pressure levels. Proposed critical values for  $q_e/q_w$  ratio are shown in Table I and Fig. 5. Results obtained with this method of CHF detection are presented in section 4.7.

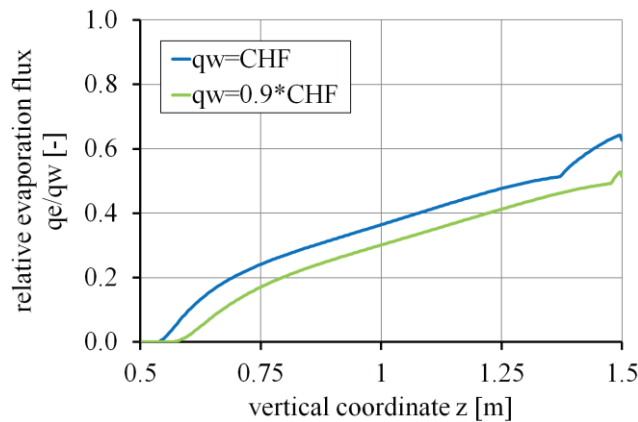
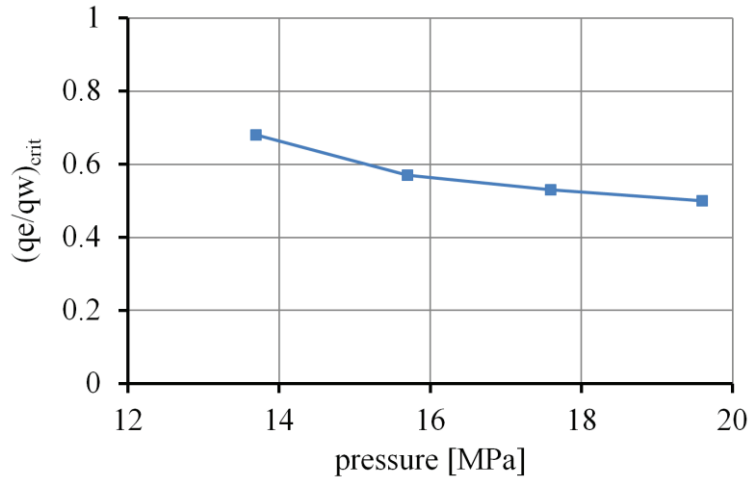


Figure 4. Case 1: Change in relative evaporation heat flux  $q_e/q_w$  as total wall heat flux  $q_w$  increases

Table I. Proposed dependence of CHF criterion on pressure

p [MPa]	$(q_e/q_w)_{crit}$
13.7	0.68
15.7	0.57
17.6	0.53
19.6	0.50



**Figure 5. Dependence of CHF criterion on pressure**

Grid independence test of  $q_e/q_w$  criterion for the Case 1 is shown in Table II. It can be seen that the evaporation flux is not completely grid independent on the base mesh, but the base mesh is good enough for the demonstration of the method.

**Table II. Grid independence test of  $q_e/q_w$  criterion for Case 1**

figures: $(q_e/q_w)_{max}$ [-]	$q_w = 0.9*CHF$	$q_w = CHF$
<b>base mesh</b>	0.531	0.644
<b>fine1 mesh</b>	0.519	0.635
<b>fine2 mesh</b>	0.531	0.643
<b>coarse mesh</b>	0.565	0.687

#### 4.7. Summary of Results

Selected cases from CHF tables [3-4] were simulated with NEPTUNE\_CFD V2 code. The following tables III-VI show the results for four different pressure levels. These tables provide critical heat flux as a function of the mass flux  $G$  and local equilibrium steam quality  $X_{eq}$  for given pressure. Tube diameter is 8 mm.

The ratio of calculated CHF to CHF from the tables [3-4] is displayed by color. See color scale next to the table. Green color in the tables means that the critical heat flux was predicted with  $\pm 10\%$  accuracy. White color means that the case was not calculated. Asterisk (\*) in the table indicates that there was some problem with the case. The problem is described in "Notes". CHF criterion  $q_e/q_w$  is different for different pressures but the pressure is known a priori. CHF criterion for the given pressure is shown in every table. The prediction method worked well for a large number of cases.

**Table III. Results of simulations of CHF in pipes, pressure 13.7 MPa, diameter 8 mm**

G [kg/m <sup>2</sup> /s]	X <sub>eq</sub> [-]					CHF <sub>calc</sub> /CHF <sub>tab</sub>
	-0.3914	-0.2763	-0.1503	-0.065	0	
500	3.9	3.45	3	2.7	2.55	1.2-1.3
750	4.1	3.65	3.15	2.8	2.5	1.1-1.2
1000	4.5	3.95	3.4	3.05	2.8	1.0-1.1
1500	5.3	4.5	3.8	3.25	2.95	0.9-1.0
2000	6.15	5.15	4.15	3.5	3.1	0.8-0.9
2500	6.75	5.7	4.5	3.75	3.25	0.7-0.8
3000	7.55*	6.3	4.9	4	3.4	
4000	9.25	7.4	5.7	4.65	3.8	
5000	10.6**	8.45	6.4	5.3	4.3	

Figures: CHF<sub>tab</sub> [MW/m<sup>2</sup>]

Notes on Table III:

\*) Calculation crashes on the base mesh at  $qw = 0.85 \cdot CHF_{tab}$ . CHF<sub>calc</sub> = 0.9 · CHF<sub>tab</sub> on the coarse mesh.

\*\*\*) Calculation crashes on the base mesh already at  $qw = 0.8 \cdot CHF_{tab}$ . On the coarse mesh,  $qe/qw = 0.67$  at  $qw = 0.95 \cdot CHF_{tab}$ . Calculation crashes at  $qw = CHF_{tab}$ .

**Table IV. Results of simulations of CHF in pipes, pressure 15.7 MPa, diameter 8 mm**

G [kg/m <sup>2</sup> /s]	X <sub>eq</sub> [-]					CHF <sub>calc</sub> /CHF <sub>tab</sub>
	-0.4737	-0.339	-0.1892	-0.0845	0	
500	2.95	2.55	2.2	1.85	-	1.2-1.3
750	3.3	2.9	2.45	2.15	2	1.1-1.2
1000	3.75	3.25	2.7	2.35	2.1	1.0-1.1
1500	4.55	3.8	3.25	2.75	2.3	0.9-1.0
2000	5.4	4.5	3.65	3	2.45	0.8-0.9
2500	6.1	5.05	4.05	3.35	2.65	0.7-0.8
3000	6.8	5.65	4.45	3.6	2.85	
4000	8.3	6.7	5.25	4.25	3.15	
5000	9.8*	7.85	5.9	4.7	3.75	

Figures: CHF<sub>tab</sub> [MW/m<sup>2</sup>]

Notes on Table IV:

\*) Calculation crashes at  $qw = 0.85 \cdot CHF_{tab}$  on the base mesh. CHF criterion is exceeded at  $qw = 0.85 \cdot CHF_{tab}$  on the coarse mesh.

**Table V. Results of simulations of CHF in pipes, pressure 17.6 MPa, diameter 8 mm**

G [kg/m <sup>2</sup> /s]	X <sub>eq</sub> [-]					CHF <sub>calc</sub> /CHF <sub>tab</sub>
	-0.5952	-0.4332	-0.2501	-0.1174	0	
500	2.2	1.9	1.65	1.5	1.4	1.2-1.3
750	2.95	2.5	2.1	1.75	1.5	1.1-1.2
1000	3.45	2.85	2.25	1.9	1.6	1.0-1.1
1500	3.7	3.2	2.55	2.25	1.8	0.9-1.0
2000	4.6	3.75	3	2.5	2.1	0.8-0.9
2500	5.05	4.35	3.3	2.8	2.15	0.7-0.8
3000	5.7	4.7	3.55	3	2.35	CHF criterion: qe/qw = 0.53
4000	7.25	5.75	4.4	3.55	2.85	
5000	8.7*	6.85	4.95	3.85	3.05	

Figures: CHF<sub>tab</sub> [MW/m<sup>2</sup>]

Notes on Table V:

\*) At qw = 0.9·CHF<sub>tab</sub>, qe/qw = 0.524, i.e. just below the CHF criterion. Calculation crashes at qw = 0.95·CHF<sub>tab</sub> on the base mesh.

**Table VI. Results of simulations of CHF in pipes, pressure 19.6 MPa, diameter 8 mm**

G [kg/m <sup>2</sup> /s]	X <sub>eq</sub> [-]					CHF <sub>calc</sub> /CHF <sub>tab</sub>
	-0.8415	-0.6277	-0.3815	-0.195	0	
500	1.7	1.55	1.45	1.35	1.3	1.2-1.3
750	2.05	1.8	1.6	1.4	1.35	1.1-1.2
1000	2.3	2.05	1.75	1.55	1.35	1.0-1.1
1500	2.95	2.55	2	1.8	1.5	0.9-1.0
2000	3.55	2.85	2.4	2	1.65	0.8-0.9
2500	4.05	3.45	2.65	2.2	1.75	0.7-0.8
3000	4.95	3.75	3	2.35	1.9	CHF criterion: qe/qw = 0.50
4000	6.25	4.85	3.55	2.65	2	
5000	7.55	5.8	4.05	3	2.3*	

Figures: CHF<sub>tab</sub> [MW/m<sup>2</sup>]

Notes on Table VI:

\*) At qw = 1.2·CHF<sub>tab</sub>, qe/qw = 0.496, i.e. just below the CHF criterion.

## 5. CONCLUSIONS

New version of NEPTUNE\_CFD code (V2.0.1) with new set of models of physical phenomena in boiling flow was tested against data from the tables of critical heat flux in tubes. It was found out that CHF criterion based on void fraction = 80% does not work well with new models in NEPTUNE\_CFD V2. But it was discovered that the CHF criterion can be based on ratio of [evaporation heat flux/total wall heat flux]. Evaporation heat flux is one of the four heat fluxes calculated by the extended Kurul and Podowski wall boiling model. Critical value of [evaporation heat flux/total wall heat flux] ratio depends on the

pressure. The proposed method of CHF prediction was tested on four different pressure levels (13.7 MPa, 15.7 MPa, 17.6 MPa and 19.6 MPa) and it worked well in many cases. The method does not work for low mass flux cases (1000 kg/m<sup>2</sup>/s or 750 kg/m<sup>2</sup>/s and below, depending on pressure).

Problems with numerical stability of the code were encountered in cases with extremely high critical heat flux (cases with high mass flux and low subcooling). These problems could be partially resolved by the use of coarser mesh. These problems were more severe for lower pressure cases.

## NOMENCLATURE

CFD	computational fluid dynamics
CHF	critical heat flux
CHF <sub>calc</sub>	critical heat flux calculated by the NEPTUNE code [MW/m <sup>2</sup> ]
CHF <sub>tab</sub>	critical heat flux given by the tables [MW/m <sup>2</sup> ]
D	tube diameter [m]
DNB	departure from nucleate boiling
G	mass flux [kg/m <sup>2</sup> /s]
L	tube length [m]
p	pressure [Pa]
q <sub>e</sub>	evaporation heat flux on the wall [MW/m <sup>2</sup> ]
q <sub>w</sub>	total wall heat flux [MW/m <sup>2</sup> ]
X <sub>eq</sub>	equilibrium steam quality [kg/kg]

## ACKNOWLEDGMENTS

Presented work was carried out within the 7<sup>th</sup> FP EURATOM NURESAFE project. NEPTUNE\_CFD V2 code is being developed by EDF, CEA, AREVA and IRSN in France. The code is implemented in the NURESIM platform.

The research leading to these results is partly funded by the European Atomic Energy Community's (Euratom) Seventh Framework Programme FP7/2007-2011 under grant agreement n°323263.

## REFERENCES

1. *NEPTUNE CFD version 2.0.1 Theory Guide*, EDF R&D Fluid Dynamics, Power Generation and Environment Department Multi-Phase and Reactive Flow Group, Chatou, France (2013).
2. *NEPTUNE CFD version 2.0.1 User Guide*, EDF R&D Fluid Dynamics, Power Generation and Environment Department Multi-Phase and Reactive Flow Group, Chatou, France (2013).
3. "Tabular data for calculating burnout when boiling water in uniformly heated round tubes", *Teploenergetika*, **23**(9), pp. 90-92 (1976), Translation in *Thermal Engineering*, September 1977, pp. 77-79 (1977).
4. J.G. Collier, *Convective Boiling and Condensation*, Second Edition, pp. 261-264, McGraw-Hill (1981).
5. G.F. Hewitt, D.N. Roberts, "Studies of two-phase flow patterns by simultaneous flash and X-ray photography". AERE-M2159 (1969).
6. N.E. Todreas, M.S. Kazimi, *Nuclear Systems I. Thermal Hydraulics Fundamentals*, pp. 469, Taylor & Francis (1993).
7. L. Vyskocil, J. Macek, "CFD Simulation of Critical Heat Flux in a Tube", *CFD4NRS-3: CFD for Nuclear Reactor Safety Applications*, OECD/NEA & IAEA Workshop, Bethesda, MD, USA, Sept. 14-16 (2010).

8. B. Koncar, C. Morel, S. Mimouni, L. Vyskocil, M.C. Galassi, “CFD Modeling of Boiling Bubbly Flow for DNB Investigations”, *Multiphase Science and Technology*, **23** (2–4), pp. 165–222 (2011).
9. M. Guingo: *Validation Note of NEPTUNE\_CFD 2.0 for NURESAFE Members*, NEPTUNE\_CFD Development Team, EDF R&D / Dept. MFEE, 6 quai Watier, 78401 Chatou CEDEX, France (2014).
10. S. Mimouni, F. Archambeau, M. Boucker, J. Lavieville, C. Morel, “A second order turbulence model based on a Reynolds stress approach for two-phase boiling flow. Part 1: Application to the ASU-annular channel case”, *Nuclear Engineering and Design* **240**, pp. 2233-2243 (2010).
11. C.G. Speziale, S. Sarkar, T.B. Gatski, “Modelling the pressure-strain correlation of turbulence: an invariant dynamical systems approach”, *Journal of Fluid Mechanics*, **227**, pp. 245-272 (1991).
12. H.C. Ünal, “Maximum bubble diameter, maximum bubble growth time and bubble growth rate during subcooled nucleate flow boiling of water up to  $17.7\text{MN/m}^2$ ”, *Int. J. Heat Mass Transfer* **19**, pp. 643-649 (1976).
13. M. Ishii, N. Zuber, “Drag coefficient and relative velocity in bubbly, droplet or particulate flows”, *AIChE Journal*, **25**(5), pp. 843-855 (1979).
14. N. Zuber, “On the dispersed two-phase flow in the laminar flow regime”, *Chemical Engineering Science*, **19**, pp. 897 (1964).
15. A. Tomiyama, H. Tamai, I. Zun, S. Hosokawa, “Transverse migration of single bubbles in simple shear flows”, *Chemical Engineering Science*, **57**(11), pp. 1849-1858 (2002).
16. P. Ruyer, N. Seiler, M. Weiss, F.P. Weiss, “A bubble size distribution model for the simulation of bubbly flows”, *Proceedings of the 6th International Conference on Multiphase Flows*, Leipzig, Germany (2007).